Topographic Mapping Using a Multibeam Radar Altimeter

Chester L. Parsons, Edward J. Walsh, *Member, IEEE,* and Douglas C. Vandemark, *Member, IEEE*

Abstract—**An airborne radar altimeter operating at 36 GHz is uniquely capable of measuring the topography of water, land, and ice surfaces. The Multimode Airborne Radar Altimeter (MARA) was designed to combine a narrow transmitted pulsewidth, a high transmitted power level, and a narrow antenna beam to produce a high-precision ranging capability at the nadir of the aircraft platform and at four fixed off-nadir angles out to 12° in the multibeam mode described in this paper, or a single beam scanning between ±22° in the scanning radar altimeter mode. Data collected over water and land surfaces are presented to demonstrate the potential of MARA for topographic mapping with accuracies and precisions of value in dynamic oceanography, geodesy, geology, hydrology, biogeochemistry, biogeography, and glaciology.**

I. Introduction

THE Multimode Airborne Radar Altimeter (MARA) is a 36-GHz radar altimeter developed by the NASA Goddard Space Flight Center Wallops Flight Facility (WFF) to map the earth's topography with high precision. It was designed with a high degree of flexibility for a variety of remote sensing disciplines in the Earth Observing System (EOS) era. Potential applications for hydrology, biogeochemistry, biogeography, ecology, geology, geophysics, oceanography, and glaciology levied measurement requirements that were factored into the MARA design. These design requirements are discussed by Parsons [2]. For all these potential applications, the capability to gather high-precision topographic measurements over a wide swath of illumination is an important attribute. An area of land, water, or ice can be surveyed much more quickly and inexpensively if the radar system's transmitted beam pattern is not restricted to the aircraft platform's nadir, which has been the case for radar altimeters developed to date. The key engineering development incorporated in the MARA design is a wide swath illumination capability.

MARA has two modes, a multibeam mode (MM) and a scanning radar altimeter mode (SRAM). Both achieve the desired wide swath coverage but through differing approaches. The MM produces five transmitted beams that are fixed in angle in flight but which can be oriented at different off-nadir angles out to a maximum of 12°. The SRAM generates a single transmitted beam, which is scanned in the cross-track direction. With the aircraft's forward motion the MM produces strips of topographic information with a high density of pulses, while the SRAM maps the topographic data within its swath in image form, but with only one radar pulse per pixel. Except for the antenna subsystem, the two modes are basically identical. The other subsystems in the two modes essentially share the same components. Detailed discussion of the SRAM will be presented in a separate paper.

This paper describes the MM design and gives examples of the information obtained using the MARA fixed beam mode. One of the benefits of this real-aperture radar system is the ease and speed with which its data can be processed. Radar range, backscattered power, and waveform data can be processed and made available for analysis within hours after a data collection mission.

Manuscript received April 1, 1991.

The authors are with NASA Goddard Space Flight Center, Laboratory for Hydrospheric Processes, Wallops Flight Facility, Wallops Island, VA USA.

E. Walsh is presently on assignment at the NOAA Environmental Technology Laboratory, R/E/ET1, Boulder, CO 80303 USA.

IEEE Log Number 9405535.

II. Instrument System

A. Antenna Subsystem

Bush *et al.* [1], Parsons [2], Parsons and Walsh [3], and Brown *et al.* [4] discuss the problems of off-nadir high-precision radar altimetry. Off-nadir illumination angles result in a spreading of the backscattered waveforms and subsequent loss of precision in the measurement of surface heights. To counter this effect, the beamwidth must be reduced. MARA was designed to operate as a beam-limited rather than pulse-limited radar. Barrick [5] defines a radar to be in beam-limited operation when the curvature effects of the spherical earth and the spherical transmitted pulse are negligible. That is, the interaction of the electromagnetic pulse with the surface occurs along a plane.

A large-aperture dielectric lens was selected as the MARA antenna to insure beam-limited operation at the operating altitudes of the WFF P-3 research aircraft. Use of a lens also allows versatility in configuring multiple-beam, near-nadir angle pointing configurations. The MM lens is described by Parsons and Miller [6]. It is fabricated from Rexolite 1422 material and has an aperture diameter of 85.6 cm and focal length of 96.3 cm. Fig. 1 shows the MM antenna assembly mounted in the P-3 bomb bay. The fairing was designed and built in-house to reduce lens structure drag during flight.

The one-way beamwidth of the lens is 0.62° on axis. When illuminated by an off-axis feed, the exit beam from the lens is directed off axis. The beam cross section becomes slightly asymmetric with increasing off-axis angle. Essentially, the transmit beam suffers from astigmatism. At 12°, the beamwidth in the plane perpendicular to the plane containing the scanned beam and lens axis increases from 0.62° to 0.95°. This astigmatism is responsible for a restriction to off-axis

Fig. 1. The installation of the MARA MM lens antenna and fairing in the forward bomb bay of the P-3. (The white blade antenna mounted on the fairing is for an aircraft system.)

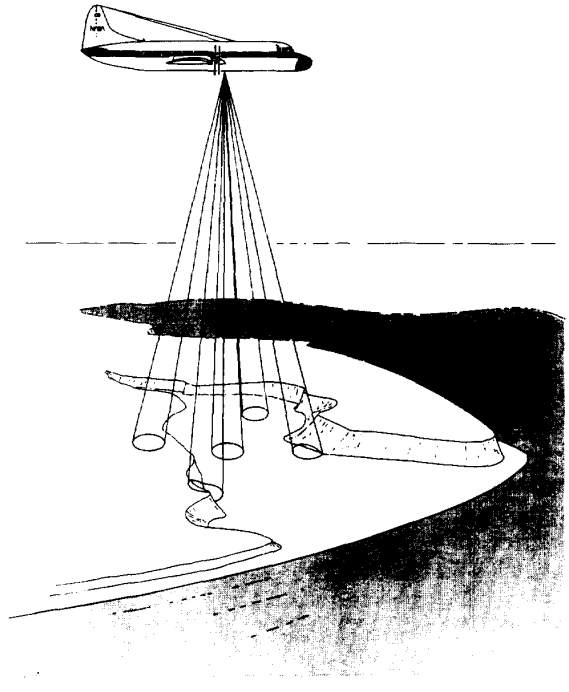

Fig. 2. Schematic illustration of the NASA P-3 aircraft and the MARA multibeam mode beam configuration over a complex surface.

angles less than 12°. On axis, the antenna's directive gain is 47.4 dB, which decreases to 45.6 dB at 12° off-axis.

For MM operation, the lens is illuminated by five feeds, one on-axis beam and four quadrature off-axis beams with exit angles of up to 12° off axis. The MM beam configuration is shown schematically in Fig. 2. Off-axis angles can be adjusted between 0° and 12°, but are fixed inflight.

As discussed by Parsons and Miller [6], the experimentally optimized feed locations for scan angles out to 20° can be approximated by a cubic equation. Using such a description, the computed and experimentally determined locations can be compared. At a given location in the lens radial direction, the average difference between computed and measured axial focal plane positions is 0.25 cm. The standard deviation of the differences is 0.5 cm, which is on the order of the measurement accuracy possible on the antenna range used.

MM antenna pattern measurements show that the beam exit angle is 0.88 of the feed illumination angle. The ratio of feed illumination and exit beam angles computed using ray tracing and the equations of the lens front and back surfaces was in good agreement with this experimental result. Newkirk and Brown [7] have developed an algorithm to model the shape of the off-axis beams and the average return power waveforms.

B. RF Transmitter Subsystem

The RF transmitter subsystem consists of two main elements, frequency generation components at X-band and pulse-forming and amplification components at Ka-band. The system block diagram is shown in Fig. 3. A crystal oscillator drives two phase-locked oscillators, one at 9.0 GHz and one at 8.85 GHz. The 9.0 GHz signal is multiplied up to 36.0 GHz, the transmitted frequency. The 8.85 GHz signal is multiplied up to 35.4 GHz to provide local oscillator signal (LO) for the receiver mixers. Two high-speed PIN diode switches in series are used to produce the desired 4 ns pulse. The switches are driven by a TTL level pulse generated by a custom pulse-forming network. The narrow 36.0 GHz pulse is amplified by an InP solid-state preamplifier, resulting in a 250 mW signal supplied to a Varian Extended Interaction Klystron (EIK) power amplifier. This EIK has a saturated gain of 40.1 dB, a saturated output power of 1727 W for a drive power level of 170 mW, and an efficiency of 19.8%. The amplifier is controlled by a switching high-voltage modulator which turns the tube on prior to input RF drive application and holds it on past the end of the drive pulse to minimize the effects of the tube's finite rise and fall times. The transmitted pulse shape is slightly broadened by the power tube, but a transmitted pulse width (3 dB) of 6.5 ns has been achieved. The device supports a maximum PRF of 20 KHz and pulsewidth of 2 μs. The nominal MM PRF is 100 Hz.

The MM PRF generator controls the timing of the EIK modulator and receiver protection switches in the receiver/tracker subsystem. After confirmation that all five protection switches have been activated by the PRF signal, a transmit trigger signal is supplied to the EIK. A sample of the high-power transmit pulse is coupled off to trigger the receiver/tracker's high-resolution time counter used to measure the range to the surface. Finally, the high-power transmit pulse is applied to the five MM antenna feed horns through a 5-way waveguide splitter. A waveguide switch at the EIK output allows the reduction of transmit power by routing the signal through a variable attenuator.

C. Receiver/Tracker Subsystem

After backscattered MM return pulses are received through the dielectric lens by the transmit feed horns, circulators route the signals to five closely situated mixer/preamp units where

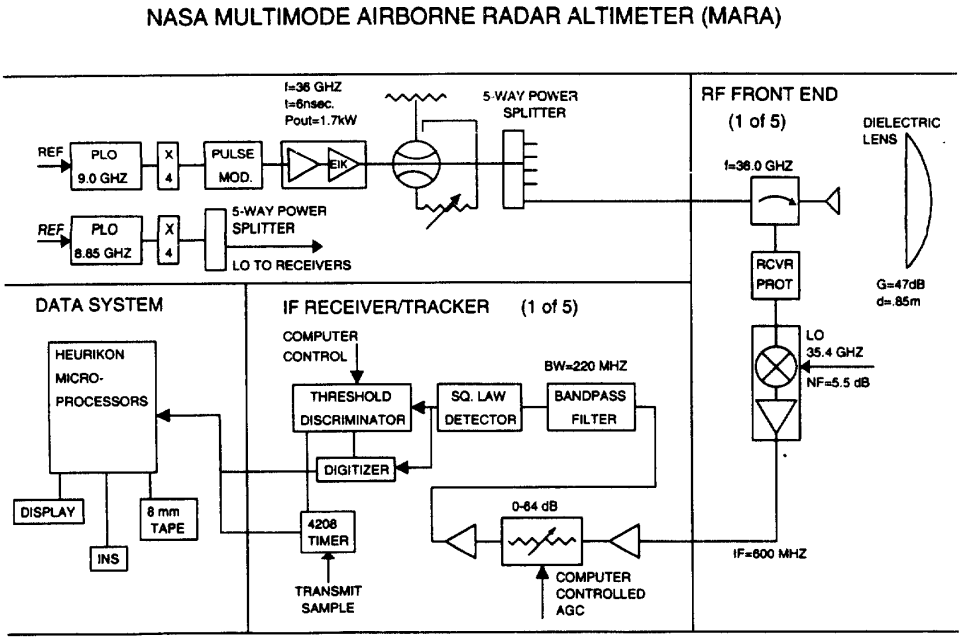

Fig. 3. Block diagram of MARA multibeam mode.

they are downconverted to an IF (intermediate frequency) of 600 MHz and amplified. The mixer/preamp units have a nominal noise figure of 5.5 dB. Following IF amplification, each of the IF signals passes through its own digitally controlled 64-dB step attenuator, set in increments of 0.25 dB. The attenuators close computer-controlled automatic gain control (AGC) loops for each of the five beams, or channels. The receiver bandwidth is 220 MHz and video detection is performed with tunnel diode square-law detectors. The nominal MM receiver noise figure is 8.2 dB, the noise floor at 290° K is −81 dBm. Experimental results confirm this figure. System dynamic range is about 60 dB as determined by front-end mixer saturation.

Digitization of the returned pulse and elapsed time (range) measurement are initiated on receipt of the surface return. The video signals are supplied in parallel as inputs to five discriminators are Lecroy 6880 digitizers. The signal amplitude at the discriminator for a particular beam must exceed some threshold level, which is set under computer control, before it will fire and its 6880 captures the return waveform. The triggered discriminator activates the digitization process and stops the elapsed time measurement for its particular beam in a Lecroy 4208 multistop time-to-digital converter.

The five 6880 digitizers are mounted in a computer assisted measurement and control (CAMAC) bus standard crate. The 4208, the discriminators, the threshold drivers, the AGC drivers, and a peripheral device interface are contained in a second CAMAC crate. Time of day, the output of a vertically mounted accelerometer, and analog pitch and roll data are supplied to the MARA data subsystem through the peripheral device interface.

The digitizers are key to the MARA performance. The Lecroy units have a digitization rate of 1.3 giga samples/s and a 3 dB full-power analog bandwidth of 250 MHz, which matches the spectral width of the EIK. The 6880 has a pretrigger range of 7.4 μs. This allows digitization and storage of waveform samples occurring prior to the discriminator's threshold detection, documenting the complete backscattered waveform.

Calibration of the digitizers is an important function of the MARA data subsystem. Each digitizer uses a bank of 32 charge coupled devices (CCD) that are highly linear, but each must be characterized by unique gain and bias coefficients calibrated before data collection periods. For extended missions, this calibration procedure must be repeated periodically because the calibration is affected by temperature and the equipment is not temperature controlled.

D. Data Subsystem

MARA's data subsystem uses a distributed, multiprocessor computer system to perform the various functions required for MM operations. The multiprocessor consists of four single-board Heurikon microprocessors housed in a Multibus card cage along with a 4 Mb memory card and a tape interface card. One microprocessor, operating in UNIX, provides a user interface and controls writing of data to an 8 mm tape drive. The other three operate in VRTX, a real-time operating system. The first of these processors acquires the peripheral device data from the ancillary data CAMAC crate and closes the AGC loop. It also acquires aircraft digital inertial navigation system (INS) data through an SEX interface card. INS data include

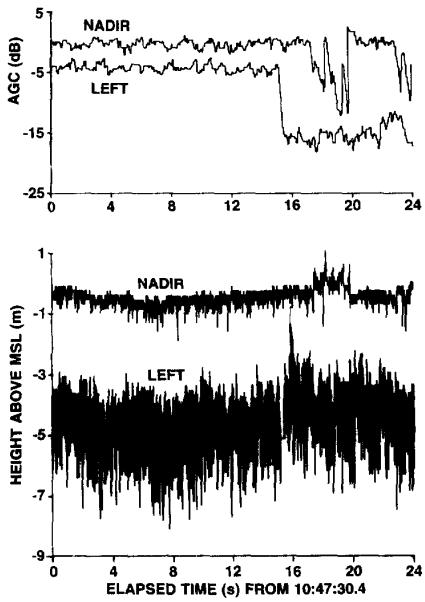

Fig. 4. Nadir and left beam AGC and height from pitch and roll corrected slant ranges over Chincoteague Bay on 1/18/90.

latitude and longitude, aircraft ground speed, yaw, and other important information. A second VRTX board acquires the digitized waveform information from the five 6880s. It is also responsible for calibrating these waveforms in real time. The third VRTX board controls a real-time EGA display.

The majority of the system software is written in the C language. The most notable exceptions are the calibration routines for the waveform acquisition processor, which are written in assembler. All programming is stored on a 155 Mb hard disk interfaced to the UNIX processor.

III. Performance

A. Threshold Detection Ranging Noise

Fig. 4 contains time series of AGC and surface elevation from threshold-detected range for the nadir and left beams acquired on January 18, 1990, during a flight over Chincoteague Bay, a sheltered body of water next to WFF (37.94°N, 75.46°W) on the Virginia coast. The 10:00 and 11:00 EST wind observations at WFF were 3.6 and 3.1 ms^{-1}, both from 190°. With the wind light, the bay surface acted as a flat, slightly rough reflector.

The aircraft altitude was about 1.7 km and the threshold range values were corrected for aircraft pitch and roll and for the nominal 12° boresight angle for the off-nadir channel. Since the left beam indicates the water surface is about 4 m lower than for the nadir beam, it is apparent that the beam pointing angles were not at their nominal values. More-precise aircraft-leveling corrections will be described in the next section. For the first 15 s all the beam footprints were over the bay, and there was little variability in the AGC records. The fluctuations in AGC after that are due to encounters with marshland bordering the bay and will be discussed later.

Since the MARA operates monostatically, the two-way 0.44° beamwidth produces a nadir footprint of about h/131, where h is the aircraft altitude. The range extent of the 13-m footprint in this instance is negligible at nadir, but is 2.8 m at 12° off-nadir, almost three times the pulse half-power width. The standard deviations of the range data for this same period were 0.21 and 1.02 m, respectively. The standard deviations for the forward and right beams were 0.81 m and 1.01 m. The off-nadir viewing angle resulted in about a 4.5:1 increase in the range noise level. The range noise increase results from the broadening of the MARA's electromagnetic pulse upon scattering from the bay surface at the off-nadir viewing geometry.

The nadir standard deviation is limited by the resolution of the time-to-digital counter used to measured the two-way transit time. For this data set the resolution was 1 ns, or equivalently 0.15 m, which is a substantial portion of the computed result. Better height measurement precision would result if a counter with higher time resolution were installed in the system.

B. Attitude Angle and Mounting Bias Effects

For the fixed-beam MM, the angle of interception of a beam with the surface is critical, as seen in the previous section. During the mechanical alignment of the feed horns in the antenna assembly, the angles of the off-axis feeds were set to 13.6°, presumably yielding angles from the lens of 12° for all four quadrature beams. A nominal 2° pitch angle toward the tail of the aircraft was designed into the MARA antenna mount to compensate for the tendency of the P-3 to fly in a 2° nose-up attitude. Installing the antenna in the P-3 bomb bay can also introduce bias in the pointing angles for the five beams.

Fig. 5 shows an expansion of the Fig. 4 data segment from 8 to 11 s containing threshold detection ranges. The average nadir range measurement for this segment was 1706.14 m, and the slant ranges for the other beams were 1741.24 m (forward), 1746.26 m (right), and 1748.44 m (left). The aft channel was not functioning. As with any radar system, all four channels evidence data dropouts due to the scintillating return occasionally being too weak to cross the threshold.

In addition to the pitch and roll data from the aircraft INS, corrections are required to account for uncertainties in the actual boresight angles for the beams, for mounting bias angles from the installation, and for possible biases in the INS attitude angle data. It is not necessary to determine the individual bias contributions to the orientation of each beam since only their composite affects the measurements. They can be systematically calculated from ranging data acquired over a flat surface, and the Chincoteague Bay determinations are given in Table I. They indicate that the forward and right beams were displaced 12.45° from the nadir beam, and the left beam was displaced 12.47°, a nearly perfect symmetry.

With these bias angles and the INS pitch and roll attitude angles, the four operative beams produced mean measured heights within 1 cm of 1705.94 m for the Fig. 5 data segment. This technique could be extended to level the instrument to

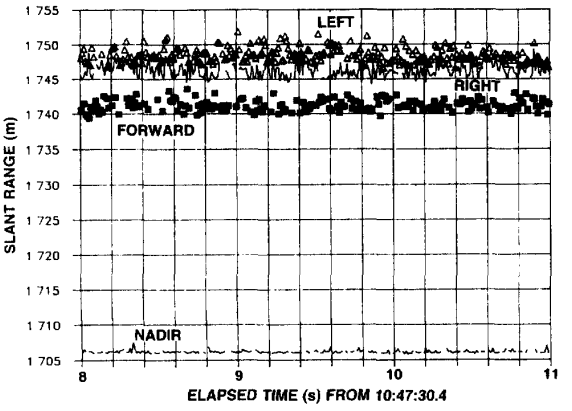

Fig. 5. A 3-s time series of raw slant range measurements from the forward, right, nadir, and left beams during the Chincoteague Bay overflight on 1/18/90.

TABLE I
MARA BEAM POINTING ANGLES

Beam	Pitch angle	Roll angle
Forward	10.84°	0.16°
Right	−1.61°	−12.29°
Nadir	−1.61°	0.16°
Left	−1.61°	12.63°

sub-centimeter accuracy. Since the MM antenna is removed between operations, the attitude angle biases may not be constant from one mission to the next. However, they can be determined for each mission as demonstrated above.

C. Average Backscattered Waveform Shapes

The range noise increase in signals backscattered from off-nadir relative to nadir relates to their mean width. Fig. 6 shows the average of nine consecutive pulses from the nadir beam at 14:18:05 when the aircraft was at 2932 m altitude over Chincoteague Bay on December 1, 1989. The amplitudes are in units of digitizer counts, proportional to received power. The 6.5 ns transmitted pulse has a half-power width of 0.98 m, and the half-power width of this nadir-beam average return is only 1.04 m, nearly identical to the transmitted pulse. There is a negative bias in the digitizer, and the oscillation apparent in the 1 to 5 m range interval is the receiver response of the wide bandwidth system.

Fig. 7 shows 0.75-s averages (about 50 pulses with the dropouts) for the return waveforms from the forward, right, and left beams about 3 s prior to the data of Fig. 6. These waveforms have been adjusted to correspond to 33.25 dB on the IF attenuators. The aircraft altitude was less than 1 m different than for Fig. 6, but small changes in the aircraft pitch and roll separated the slant ranges of the three beams making the return waveforms easier to distinguish. The fluctuations in the right beam return signal in the 3015 to 3025 m range interval indicate the intrinsic noisiness of the Lecroy 6880 digitizer used for that channel. The degree of noisiness of the 6880s is monitored between missions, and the least noisy unit is used for the nadir channel. The pretrigger ranges of the digitizers were not set properly and part of the leading edge of the waveforms were lost.

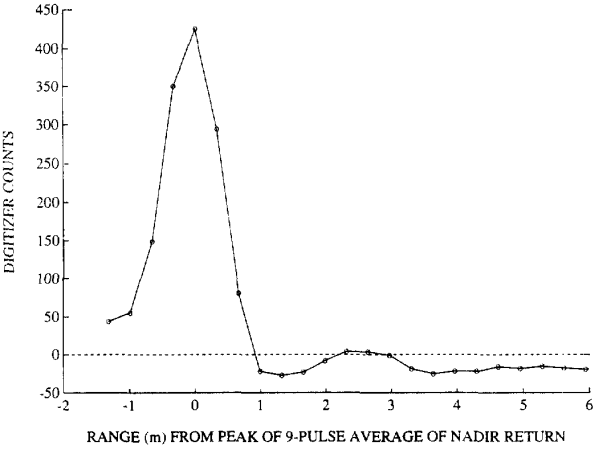

Fig. 6. Average of nine consecutive return waveforms from the nadir beam at 2932 m height over Chincoteague Bay on 12/1/89.

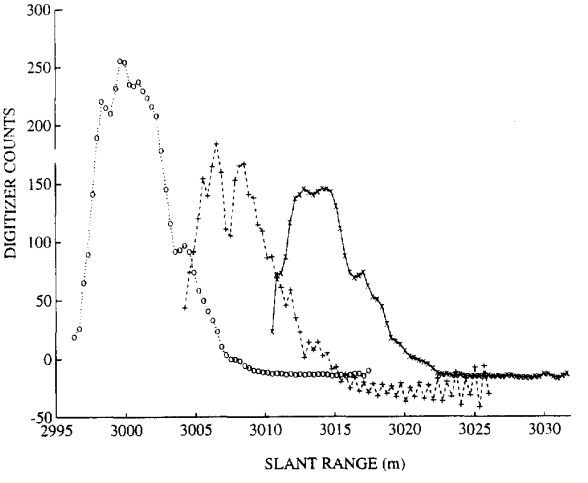

Fig. 7. Approximately 50-pulse averages from the left (o), right (+), and forward (x) beams at 2932 m height over Chincoteague Bay on 12/1/89.

The half-power widths of these returns for the left, right, and forward beams are 6.09, 6.23, and 6.05 m, respectively. Although their widths are nearly identical, the amplitudes of the returns diminish as the slant range (off-nadir angle) increases, indicating the falloff of sigma naught with increasing incidence angle. When the central beam was pointing nearly at nadir 3 s later (Fig. 6), the slant ranges of the three off-nadir beams approached 3003 m and their peak values approached 230 counts. The peak count for the nadir return of Fig. 6 is only about 2 dB higher than the peak count for the left beam in Fig. 7. But the IF attenuator reference level for Fig. 6 was 8 dB higher, so the nadir return power was more than 10 dB higher than the power at 12.5° off-nadir.

The off-nadir geometry resulted in about a 6:1 increase in the average width of the backscattered waveform compared to the transmitted pulse. That result can be compared with a rudimentary calculation of expected waveform width based on the geometry. Parsons [2] indicates that the off-nadir range extent of the half-power width of the antenna pattern is

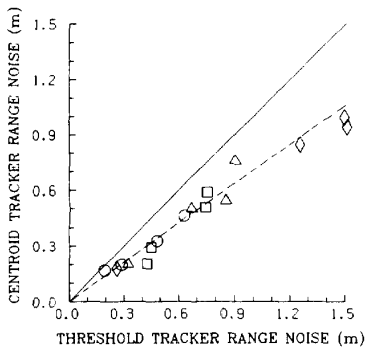

Fig. 8. Comparison of the standard deviations of the residuals after detrending for the threshold and centroid trackers. The circles represent data at 735-m altitude, squares at 1020 m, triangles at 1460 m, and diamonds at 2920 m.

$$w = (h\phi \tan\theta)/\cos\theta \tag{1}$$

where ϕ is the two-way 3-dB beamwidth, θ is the off-nadir angle, and h is the platform altitude. For 2932-m height, 12.46° off-nadir, and a 0.44° two-way half-power antenna pattern, $w = 5.1$ m. Convolving this width with the transmitted pulse results in a slight broadening to 5.2 m. The increase in width from 5.2 to 6.1 m is due to tracking noise.

D. Centroid Tracking

The precise measurement of range may benefit from the use of the centroid of the backscattered waveform as the track point, rather than the detection of the crossing of a threshold, which the MM default track point used in the discussions thus far. Centroid range tracking was obtained by adding to the threshold range the distance from the start of the return waveform to its centroid. The average range variation was determined for the threshold ranges and for the centroid ranges using a moving 41-point simple average. The average at each position was subtracted from the midpoint range, and the standard deviations of the residuals for the threshold and centroid trackers are plotted in Fig. 8 for the first 10 s of data acquired at four different altitudes during the flight of December 1, 1989.

The range noise increases with the width of the return pulse, which in turn is dependent on the altitude, the nominal off-nadir boresight of the beams, and the pitch and roll attitudes of the aircraft. The solid line (45° slope) is where the points would lie if the centroid tracker is seen in all cases to be an improvement over the threshold tracker. The standard deviation is typically reduced by the square root of 2 (dashed line), which means that the range noise power (variance) would be cut in half using the centroid tracker.

IV. Land Mapping

The data of January 18, 1990, presented in Fig. 4 were acquired while the aircraft was proceeding on a groundtrack of 3.6° at 119.7 ms^{-1}. The latte part of the segment contains data over marshlands (38.01°N, 75.38° W) bordering Chincoteague Bay adjacent to Franklin City, VA. Fig. 9 contains an expansion of the 14 to 24 s interval of Fig. 4. The top panel shows the groundtracks for the left, nadir, and right beams superimposed on a 1:24,000 U.S. Geological Survey (USGS) map for Girdletree, MD.

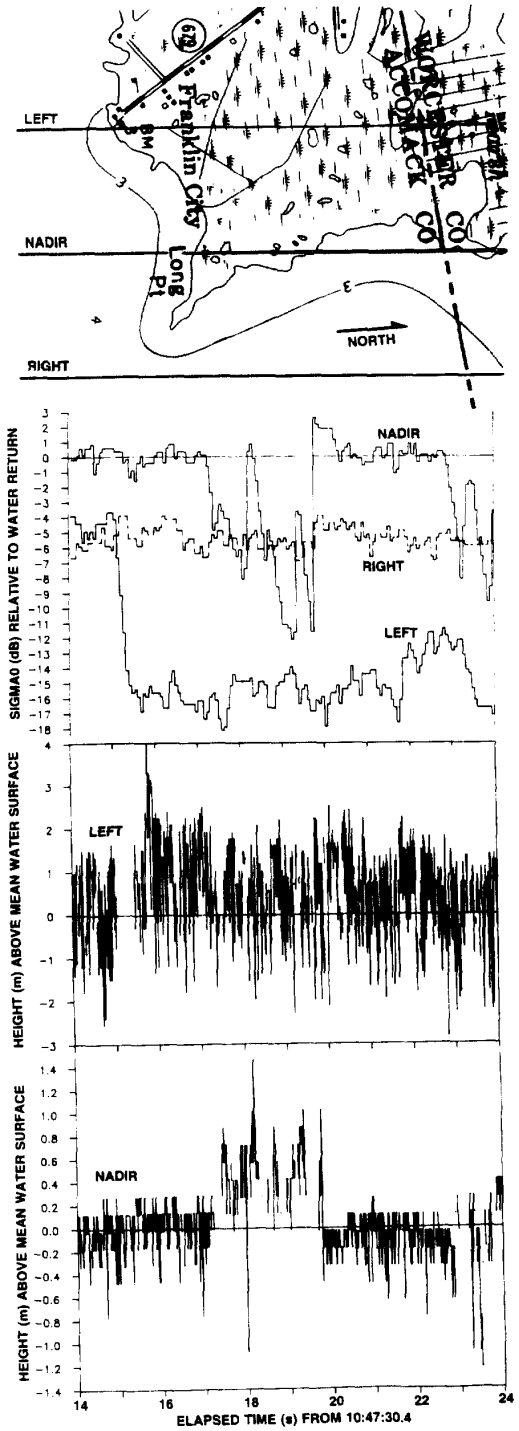

Fig. 9. The groundtracks for the left, nadir and right MARA MM beams in the vicinity of the marsh near Franklin City, VA, on 1/18/90 (top panel). Backscattered cross-section measurements for the nadir, right, and left beams relative to the nadir return from the average sea surface (second panel). Left (third panel) and nadir beam (fourth panel) measured heights above the average sea surface.

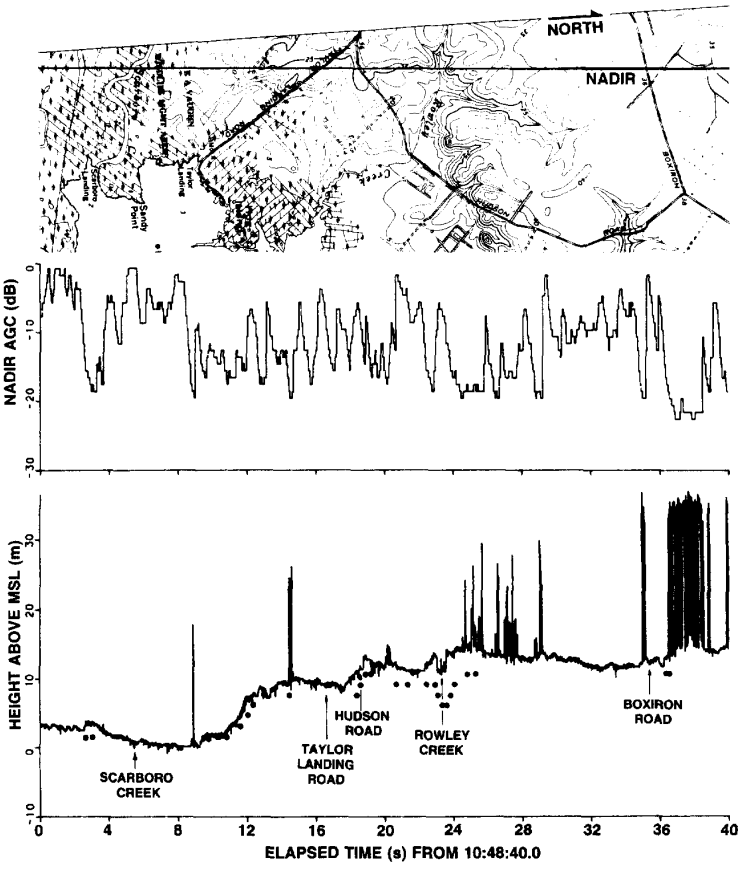

Fig. 10. Nadir beam groundtrack from Scarboro Creek, MD, to Boxiron Road on 1/18/90 (top panel). AGC (second panel) and height (third panel) measurements for the nadir channel over the Scarboro Creek area on 1/18/90. The heights of the 5 ft contour lines on the U.S. Geological Survey 1:24,000 topographic map are also plotted, along with roads and creeks of interest.

The second panel of Fig. 9 compares the AGC values from the nadir, left, and right beams. The left footprint crossed from the bay to land at about 15 s, remaining over land for the duration of the figure. The nadir footprint was over land between about 17 and 20 s, and then hit land again near the Accomack-Worcester county line. The right beam was always over Chincoteague Bay. The AGC data are all referenced to the nadir return over open water, where the left and right beams both measured about 5 dB less backscattered power than did the nadir channel. Assuming a mean square slope value of 0.018 in the backscattering cross-section model [8, 9] results in a rolloff of about 5 db between nadir and 12° off-nadir. This is a reasonable value [10] for the light winds over Chincoteague Bay during this flight.

The nadir AGC drops to a minimum of −12 dB over the marsh, a value that is consistent with the decrease seen in the left beam. The major fluctuations seen in the nadir channel over the marsh are probably due to patchy areas of standing water. The maximum change of −12 dB is consistent with the few reported measurements of radar reflectivity from grassy surfaces at the MARA's frequency.

The bottom two panels of Fig. 9 show the left and nadir beam height information. Corrections for the aircraft pitch and roll measurements have been made, and the height has been subtracted from the average height over the water so that the resultant plots are of height above the mean bay surface. The INS pitch data varied from 0.73° to 0.79°, and the roll changed between 0.04° and 0.2°. The height change caused by the marsh is evident. The height difference from water to land measured by the left beam was about 54 cm; at nadir the difference was 46 cm for the segment between 17 and 20 s. At nadir, the granularity introduced by the 1 ns resolution in the ranging time measurement is clearly evident in the bottom panel of Fig. 9. Increased noise in the off-nadir data obscures the granularity.

The aircraft groundtrack shown in Fig. 9 continued on after the Franklin City data segment, and the top panel of Fig. 10 shows the nadir track about 1 minute later, superimposed on the 1:24,000 USGS map for Boxiron, MD. It crossed Scarboro Creek (38.07° N, 75.37° W), Taylor Landing and Hudson Roads, Rowley Creek, and Boxiron Road. The AGC and height data from the nadir channel are graphed in the second and third panels of Fig. 10. The MARA data have been referenced to the minimum height measured during this segment (in the vicinity of Scarboro Creek). The divergence of the MARA profile from the map elevations indicated by the dots is no

doubt due to the aircraft altitude drifting by several m over the 40 s interval. But accelerometer data were not available so it was not possible to eliminate the aircraft vertical motion. Incrementally, the MARA profile appears excellent.

The signal from the MARA was efficiently attenuated by pine tree canopies. In Fig. 10, the clearest evidence is seen between 36.5 and 39 s elapsed time. The 36 GHz pulse rarely penetrated to the ground through a stand of 20-m trees. The backscattered cross section dropped by about 22 dB below the level backscattered from water. This attenuation is the largest found in any MARA data set examined thus far. Data for this groundtrack were also collected for the left, forward, and right beams. The attenuation caused by the pine trees was actually less for the off-nadir channels.

V. Conclusions

The height and backscattered power measurement capabilities of the MARA MM make it a useful instrument for a variety of topographic mapping applications. Its high precision is a necessary attribute for oceanographic and glaciological topography mapping. The data included in this paper are the first produced from an airborne, high-precision, beam-limited altimeter operating at nadir and off-nadir angles. The mean backscattered waveform shape as a function of viewing geometry and altitude matched expectations. The MARA MM has sufficient transmitted power to permit its use over any surface. It is an extremely capable remote sensing tool for studying beam-limited radar operations for off-nadir angles up to 12°.

The data sets presented demonstrate the usefulness of the instrument for topographic mapping. When used in conjunction with differential global positioning system (GPS) data, it should be possible to map surface relief with decimeter accuracy. This suggests that the MARA will be a valuable resource in the Eos era, when topographic information about the earth will be required by disciplines as diverse as oceanography, geodesy, geology, hydrology, biogeochemistry, biogeography, and glaciology.

Acknowledgment

The authors would like to express their thanks and gratitude to the many people who were instrumental in the development of the MARA. The requirement for beam-limited altimetry was highlighted in program planning documents by J. T. McGoogan of NASA/GSFC/WFF. Lee Miller, of Applied Science Associates, Inc., helped with the initial conceptual design of a multiple-beam radar system for aircraft applications and with the design of the dielectric lens for the system.

The following NASA/GSFC/WFF personnel were critical in the development of this system. Al Selser designed the RF sections of the instrument and Wayne Wright designed the data system. Don Hines packaged the RF components, tested the packaged units, and installed the hardware on the P-3. Charles Piazza wrote most of the system software and served as system operator during flights. John Ward designed, built, and tested the hardware interface circuitry, the timing and protective circuits, and also served as system operator. Doug Young designed the antenna housing and the fairing for the aircraft installation; Pete Bradfield and Roger Navarro assisted in flight scheduling support. Don Shirk designed and tested the waveguide runs in the transmitter. Finally, we thank Chet Koblinsky and Jim Garvin of GSFC for their interest, many fruitful discussions, and their support during the development of the radar system.

Co-Author Comment: Chester Parsons died unexpectedly shortly after submitting this paper for publication. With the increased workloads after his death, the paper was never revised in the light of the reviewers' comments. This is the first data from the system Chester conceived of and brought to fruition. The MARA is one of Chester's many legacies. He is still missed, and his programs continue.

References

[1] G. B. Bush, E. B. Dobson, R. Matyskiela, C. C. Kilgus, and E. J. Walsh, "An analysis of a satellite multibeam altimeter," *Marine Geodesy*, vol. 8, nos. 1–4, pp. 345–384, 1984.

[2] C. L. Parsons, Ed., *MARA System Documentation. Vol. I MARA System Requirements Document*, NASA Ref. Publ. 1226, 92 pp., 1989.

[3] C. L. Parsons and E. J. Walsh, "Off-nadir radar altimetry," *IEEE Trans. Geosci. Remote Sensing*, vol. 27, pp. 215–224, 1989.

[4] G. S. Brown, L. S. Miller, and L. W. Choy, "Multibeam radar altimetry: spaceborne feasibility and airborne experimentation," NRL Rep. 9229, unclassified, Naval Research Laboratory, Washington, DC 20375-5100, 32 pp., 1989.

[5] D. E. Barrick, "Determining the mean surface position and sea state from the radar return of a short-pulse satellite altimeter," in *Sea Surface Topography from Space. Volume I*, NOAA Technical Rep. ERL 228-AOML 7, chap. 16, pp. 16.1–16.19, 1972.

[6] C. L. Parsons and L. S. Miller, "Design of a large-aperture lens antenna usable over a ±15° scanning sector," *IEEE Trans. Antennas Propagat.*, vol. 36, pp. 1162–1165, 1988.

[7] M. H. Newkirk and G. S. Brown, "Issues related to waveform computations for radar altimeter applications," *IEEE Trans. Antennas Propagat.*, vol. 40, pp. 1478–1488, 1992.

[8] D. E. Barrick, "Rough surface scattering based on the specular point theory," *IEEE Trans. Antennas Propagat.*, vol. 16, pp. 449–454, 1968.

[9] D. E. Barrick, "Wind dependence of quasi-specular microwave sea scatter," *IEEE Trans. Antennas Propagat.*, vol. 22, pp. 135–136, 1974.

[10] E. Walsh, D. Vandemark, D. Hines, M. Banner, W. Chen, C. Fandry, J. Reid, J. Jensen, S. Lee, R. Swift, and J. Scott, "Wind stress versus sea surface mean square slope measured with a 36 GHz scanning radar altimeter," in *The Air-Sea Interface*," M. A. Donelan, W. H. Hui, and W. J. Plant, Eds. Toronto, Canada: Univ. Toronto Press, 1994.

Chester L. Parsons was born on March 9, 1947. He received a degree in electrical engineering from the Johns Hopkins University in 1965 and joined the Optical Systems Section at the NASA Wallops Station in Wallops Island, VA. In 1972, he enrolled in Purdue University and earned a Master's degree in Meteorology.

He returned to work at NASA in 1974 where he was assigned to the Applied Sciences Directorate. He directed the Ozone Instrumentation Intercomparison and was involved in ozone measurements from balloons and rockets. In 1981 the Wallops Flight Center was consolidated with the NASA Goddard Space Flight Center, and he was promoted to Head of the Observational Science Branch in 1984. He was Principal Investigator for the Multimode Airborne Radar Altimeter (MARA), as well as both the ROCOZ-A rocket ozone program and the Dobson spectrometer. He led efforts to provide high-quality measurements of stratospheric ozone to verify the performance of satellite-borne ozone instruments. He has authored many papers.

Mr. Parsons was a member of the American Geophysical Union, the American Meteorological Society, and Eta Kappa Nu.

Edward J. Walsh (S'60–M'74) received the B.S. and Ph.D. degrees in electrical engineering from Northeastern University in 1963 and 1967, respectively.

From 1967 to 1970 he investigated MF ducted propagation in the Earth's magnetosphere at the NASA Electronics Research Center, Cambridge, MA, both as a civil servant and a military detailee (1968–1970) as a Signal Corps officer from the U.S. Army. Since 1970 he has been with the NASA GSFC Wallops Flight Facility in Wallops Island, VA. His research interests are in the general area of remote sensing and radio oceanography, using tower-based, airborne, and satellite systems. Particular areas include the measurement and interpretation of the ocean directional wave spectrum, the sea surface mean square slope, and the variation of sea surface radar cross section as a function of parameters such as incidence angle, sea surface slope, deviation from mean sea level, wind speed, and stress.

Douglas C. Vandemark (M'88) received the B.S. in physics from Hope College, Holland, MI, in 1986 and the M.S.E.E. from the University of Massachusetts, Amherst, in 1988.

He was with the Microwave Remote Sensing Laboratory, ECE Department, University of Massachusetts from 1986 to 1988 as a research assistant and the McDonnell Douglas Helicopter Co. from 1988 to 1990 as a research engineer. In 1990, he joined the Observational Science Branch of the NASA Goddard Space Flight Center and is currently active in radar remote sensing field work and data analysis efforts directed at improving spaceborne remote sensor data interpretation. His research interests include advanced radar system design, microwave and millimeter-wave backscattering, pulse and beam-limited altimetry and ocean directional wave spectral estimation. He is currently the instrument manager for NASA's airborne Radar Ocean Wave Spectrometer (ROWS).